Biochimica et Biophysica Acta 1808 (2011) 2734–2744

Contents lists available at ScienceDirect

Biochimica et Biophysica Acta

journal homepage: www.elsevier.com/locate/bbamem

Lipid-mediated membrane binding properties of Disabled-2

Ruba Alajlouni [a], Karen E. Drahos [a,b], Carla V. Finkielstein [b], Daniel G.S. Capelluto [a,*]

[a] Protein Signaling Domains Laboratory, Department of Biological Sciences, Virginia Tech, Blacksburg, VA 24061, USA
[b] Integrated Cellular Responses Laboratory, Department of Biological Sciences, Virginia Tech, Blacksburg, VA 24061, USA

ARTICLE INFO

Article history:
Received 24 May 2011
Received in revised form 17 July 2011
Accepted 21 July 2011
Available online 27 July 2011

Keywords:
Disabled-2
PTB domain
Sulfatide
Phosphatidylinositol 4,5-bisphosphate
Micelle

ABSTRACT

Disabled-2 (Dab2) is an adaptor protein involved in several biological processes ranging from endocytosis to platelet aggregation. During endocytosis, the Dab2 phosphotyrosine-binding (PTB) domain mediates protein binding to phosphatidylinositol 4,5-bisphosphate (PtdIns(4,5)P_2) at the inner leaflet of the plasma membrane. As a result of platelet activation, Dab2 is released from α-granules and associates with both the αIIbβ3 integrin receptor and sulfatide lipids on the platelet surface through its N-terminal region including the PTB domain (N-PTB), thus, modulating platelet aggregation. Thrombin, a strong platelet agonist, prevents Dab2 function by cleaving N-PTB within the two basic motifs required for sulfatide association, a reaction that is prevented when Dab2 is bound to these sphingolipids. We have characterized the membrane binding properties of Dab2 N-PTB using micelles enriched with Dab2 lipid ligands, sulfatides and PtdIns(4,5)P_2. Remarkably, NMR spectroscopy studies suggested differences in lipid-binding mechanisms. In addition, we experimentally demonstrated that sulfatide- and PtdIns(4,5)P_2-binding sites overlap in Dab2 N-PTB and that both lipids stabilize the protein against temperature-induced unfolding. We found that whereas sulfatides induced conformational changes and facilitated Dab2 N-PTB penetration into micelles, Dab2 N-PTB bound to PtdIns(4,5)P_2 lacked these properties. These results further support our model that platelet membrane sulfatides, but not PtdIns(4,5)P_2, protect Dab2 N-PTB from thrombin cleavage.

1. Introduction

Disabled (Dab) was originally identified as a protein that plays a crucial role in *Drosophila* neural development [1]. Dab proteins contain a phosphotyrosine-binding (PTB) domain located at the N-terminus and a proline-rich SH3 domain located at the C-terminus, indicating that these proteins function primarily as adaptor proteins. Dab2 can mediate endocytosis by association with clathrin [2], the clathrin adaptor protein-2 [3], and myosin VI [4]. Moreover, Dab2 can bind to cell surface receptors that transport cargo, including the low-density lipoprotein (LDL) receptor [3], and the type 1 and 2 transforming growth factor-β receptors [5]. In addition, Dab2 binds to integrin receptors, an association that is important for coordinating changes in cell adhesion, platelet aggregation, membrane trafficking, and cell signaling [6–10].

The PTB domain belongs to the Pleckstrin Homology (PH) superfamily of structures implicated in signaling transduction, membrane trafficking, and cytoskeletal organization [11]. As defined by its name, the PTB domain was originally identified as a module that recognizes tyrosine-phosphorylated NPXY motifs [12]. However, the Dab2 PTB domain preferentially interacts with non-phosphorylated NPXY-containing proteins [13], including LDL receptor protein 1 [3] and Dishevelled-3 [14]. Dab2 PTB plays a key role in LDL receptor internalization as Dab2 co-localizes with clathrin coats on the cell membrane during endocytosis [2,3]. The three dimensional structures of mouse Dab1 and Dab2 PTB domains have been solved by X-ray crystallography in ligand-free form and in complex with both NPXY-containing peptides and phosphatidylinositol 4,5-bisphosphate (PtdIns(4,5)P_2) [15,16]. The Dab1 PTB structure contains seven central β-strands, which form two antiparallel β-sheets capped with a long C-terminal α-helix and a short N-terminal α-helix [15,16]. A basic patch on the surface of Dab1 PTB faces opposite the NPXY motif site and is involved in PtdIns(4,5)P_2 recognition [15–17]. In addition to their presence at the inner leaflet of the plasma membrane, phosphoinositides have recently been implicated in extracellular mechanisms in plant and animal cells [18]. Thus, given the ability of Dab2 to localize both intra- and extracellularly [8,19,20] and to recognize PtdIns(4,5)P_2, it is plausible that phosphoinositide recognition may be necessary for Dab2 membrane targeting on either side of the plasma membrane. The Dab2 PTB residues Lys53 and Lys90 have been shown to be critical for phosphoinositide recognition [2]; each of these lysine side chains forms hydrogen bonds with the 4- and 5-phosphates of the phosphoinositide [15].

Sulfatides, the sulfuric ester of galactosylceramides at the C3 of the galactose residue, are present in lipid rafts at the cell surface

Abbreviations: CD, circular dichroism; Dab2, Disabled-2; DDM, N-dodecyl-β-D-maltopyranoside; NMR, nuclear magnetic resonance; N-PTB, N-terminal region of Dab2 containing the PTB domain; PtdIns(4,5)P_2, phosphatidylinositol 4,5-bisphosphate; PTB, phosphotyrosine-binding domain; SPR, surface plasmon resonance

* Corresponding author at: Department of Biological Sciences, Virginia Tech, 1981 Kraft Drive, Room 2007, Blacksburg, VA 24061, USA. Tel.: +1 540 231 0974; fax: +1 540 231 3414.
E-mail address: capellut@vt.edu (D.G.S. Capelluto).

0005-2736/$ – see front matter © 2011 Elsevier B.V. All rights reserved.
doi:10.1016/j.bbamem.2011.07.029

(intracellular sulfatide concentration is ~100 nmol/g; [21]) and are thought to influence the activity of integral membrane proteins [22]. Sulfatides interact with several molecules specifically participating in hemostasis, cell adhesion, differentiation, and signal transduction [23]. Sulfatide surface levels increase upon platelet activation [24], which facilitate sulfatide binding to pro- and anti-coagulant proteins including von Willebrand Factor (vWF) [25], P-selectin [26], and Dab2 [20]. We have recently shown that the N-terminal Dab2 region containing the PTB domain (N-PTB) specifically binds sulfatides through the Lys25, Lys49, Lys51, and Lys53 residues located in two consensus sulfatide-binding motifs [20]. Sulfatide binding protects Dab2 from thrombin cleavage and sequesters it from integrin binding, partitioning Dab2 into two pools at the platelet surface and serving as a mechanism to govern Dab2 availability during platelet aggregation [20]. We have also shown that sulfatide recognition by Dab2 is required for the protein to regulate the surface expression of P-selectin, which is critical for homo- and heterotypical interactions with leukocytes [27].

Here, we describe the structural basis by which the Dab2 N-PTB region interacts with biological membranes using mimics such as micelles and liposomes enriched with Dab2 lipid ligands. We experimentally demonstrate that sulfatides and PtdIns(4,5)P_2 compete with each other for Dab2 N-PTB binding, which can be critical for cellular function when both lipids are simultaneously found in the same membrane compartment. We also show that both PtdIns(4,5)P_2 and sulfatides stabilize Dab2 N-PTB as observed by an increased tolerance of the protein to temperature-induced unfolding. Remarkably, and unlike PtdIns(4,5)P_2, sulfatides contribute to membrane penetration of Dab2 N-PTB, which is accompanied by a conformational change in the protein. Sulfatide-mediated membrane insertion of Dab2 may explain the protection of the protein from thrombin cleavage in the presence of the sphingolipid.

2. Material and methods

2.1. Chemicals

The following is a list of chemicals used and their suppliers: brain sulfatides, 1,2-dioleoyl-sn-glycero-3-phosphocholine (PC), 1,2-dioleoyl-*sn*-glycero-3-phospho-L-serine (PS), 1,2-dipalmitoyl-*sn*-glycero-3-phosphoethanolamine (PE), L-Myristoyl-2-Hydroxy-sn-Glycero-3-phosphocholine (LMPC) (Avanti-Lipids); N-dodecylphosphocholine (DPC), N-dodecyl-β-D-maltopyranoside (DDM) (Anatrace/Affymetrix); PtdIns(4,5)P_2, (Cayman Chemicals), and isopropyl β-D-thiogalactopyranoside (IPTG) (Research Products International). All other chemicals were analytical reagent grade.

2.2. Cloning, expression, and purification of Dab2 constructs

The human Dab2 N-PTB (residues 17-185) cDNA was cloned into a pGEX6P1vector (GE Healthcare). Site-directed mutagenesis of Dab2 N-PTB was performed using QuikChange (Stratagene) and proteins were expressed in *Escherichia coli* (Rosetta; Stratagene). Bacterial cells were grown in Luria-Bertani media at 37 °C until they reached an optical density of ~0.8. Induction of glutathione S-transferase (GST) fusion proteins resulted from the addition of 1 mM IPTG followed by 2-h incubation at 25 °C. ^{15}N labeled proteins were produced in minimal media supplemented with $^{15}NH_4Cl$ (Cambridge Isotope Laboratory Inc.) as the source of nitrogen. Proteins were purified using glutathione beads as described [28]. Purity of proteins was over 95% as judged by SDS–PAGE analysis.

2.3. Liposome-binding assay

Lipid mixtures were prepared as we previously described [20], and contained lipid molar ratios similar to those described in related reports [2,29]. Lipid films were generated by lyophilization and hydrated in 20 mM Tris–HCl (pH 6.8) and 100 mM NaCl to 1 mg/ml at 67 °C for 1 h and freeze-thawed three times. Liposomes were sonicated, pelleted, and suspended at 2.5 mg/ml in the same buffer. Ten μg of protein was incubated with 125 μg of total lipid for 30 min at 23 °C. Liposome-bound and free-protein samples were separated by centrifugation and analyzed by SDS–PAGE.

2.4. Circular dichroism spectroscopy

Far-UV (190–240 nm) circular dichroism (CD) spectra were recorded using a Jasco J-815 spectropolarimeter, equipped with a Jasco PFD-425 S temperature control unit at 10 μM Dab2 N-PTB in 5 mM Tris–HCl (pH 6.8), 100 mM KF, and 100 μM dithiothreitol (DTT), in the absence and presence of each of the detergent micelles under investigation (DDM, LMPC, and DPC) in their free state or enriched with either PtdIns(4,5)P_2 or sulfatides. Five CD spectral accumulations were collected at a 1-nm bandwidth with a response time of 1 s and at a scan speed of 20 nm/min at 23 °C. Buffer spectra were also acquired under the same experimental conditions and subtracted from the protein spectra before analysis. Spectra were deconvoluted to estimate the secondary structure content with the online server DICHROWEB [30] using the CDSSTR algorithm [31]. Ten accumulated near-UV CD spectra of Dab2 N-PTB (100 μM), in the absence and presence of micelles and/or lipid ligands, were collected using a 0.1-cm path length at 20 nm/min between 350 and 250 nm with a response time of 1 s and a data pitch of 0.5 nm. The temperature dependence of ellipticity at 222 nm was measured from 4 to 90 °C at 1 °C/min scan rate using 1.5 nm bandwidth and 120 s delayed time.

2.5. NMR spectroscopy

Lipid binding was monitored by comparing ^{1}H, ^{15}N heteronuclear single quantum coherence (HSQC) spectra of 200 μM ^{15}N-labeled Dab2 N-PTB in 20 mM d_{11}-Tris–HCl (pH 6.8), 100 mM KCl, 1 mM NaN_3, 1 mM d_{10}-DTT, and 10% D_2O at 25 °C on a Bruker Avance 600 MHz spectrometer. Micelle interactions were monitored by adding 250 μM DDM into samples containing 200 μM ^{15}N-labeled N-PTB and these mixtures further titrated with dihexanoyl (c6)-PtdIns (4,5)P_2 or sulfatides at the indicated molar ratios. The Dab2 N-PTB protein was also titrated with soluble c6-PtdIns(4,5)P_2 under similar experimental conditions. Spectra were processed with NMRPipe [32] and analyzed using nmrDraw [33].

2.6. Competition lipid–protein overlay assay

Lipid strips were prepared by spotting 1 μl of the indicated amount of sulfatide dissolved in chloroform:methanol:water (1:2:0.8) onto Hybond-C extra membranes (GE Healthcare). Membrane strips containing the immobilized sulfatide were blocked with buffer A [3% fatty acid-free BSA (Sigma) in 20 mM Tris–HCl (pH 8), 150 mM NaCl, 0.1% Tween-20] for 1 h at room temperature. The Dab2 N-PTB (0.1 μg/ml) protein was pre-incubated in the absence and presence of a 10-molar fold excess of the indicated phosphoinositide for 30 min at room temperature. Then, membranes were incubated with either the Dab2 N-PTB or lipid–protein mixtures in buffer A without BSA overnight at 4 °C. Following washes with the same buffer, bound proteins were consecutively probed with rabbit anti-GST antibody (Santa Cruz Biotech) and donkey anti-rabbit-horse-radish peroxidase (HRP) (GE Healthcare). Protein binding was detected using an enhanced chemiluminescence reagent (Pierce).

2.7. Surface plasmon resonance competition assay

Surface plasmon resonance (SPR) competition experiments were performed on a BIAcore X instrument using L1 sensorchips coated

with ~0.5 mM of sulfatide-containing 100 nm size-calibrated liposomes. The first flow cell was used as the control surface (liposomes without sulfatides), whereas the second flow cell (sulfatide liposomes) was employed as the active surface as described [20]. The Dab2 N-PTB binding experiments were performed in 10 mM Tris–HCl (pH 7.4) and 100 mM NaCl. This buffer was used during the equilibration, association, and dissociation phases. Dab2 N-PTB (5 μM) was pre-incubated for 20 min at room temperature in the absence and presence of dioctanoyl PtdIns(4,5)P_2 at the indicated concentrations. The free- and lipid-bound protein was then injected on both flow cell sensor chip surfaces at a flow rate of 30 μl/min. Sensorgrams were obtained for each of the indicated PtdIns(4,5)P_2 concentrations. Association and dissociation times for each protein injection were set at 120 and 600 s, respectively. Regeneration of the lipid bilayer after the dissociation phase was carried out using 20 mM NaOH.

2.8. Fluorescence spectroscopy

Intrinsic tryptophan fluorescence spectroscopy measurements were performed using a J-815 Jasco spectropolarimeter at 23 °C in a 1-cm path length cuvette. Three accumulated fluorescence spectra (310–410 nm) of Dab2 N-PTB (1 μM) in 5 mM Tris–HCl (pH 6.8), 100 mM KF, and 100 μM DTT was collected in the absence and presence of DDM micelles and/or lipid ligands using an excitation wavelength of 295 nm. Acrylamide quenching was obtained by increasing the concentration of acrylamide in the protein sample from 12.5 to 500 mM. The Stern–Volmer constant (K_{sv}) was determined using the following equation:

$$F^{\circ} / F = K_{sv}[Q] + 1$$

where F° and F are the fluorescence intensities of the sample in the absence and presence of the quencher, respectively, and [Q] is the molar concentration of the quencher [34].

2.9. Statistical analysis

Statistical analysis was conducted using Kaleidagraph, version 4.03, Synergy software. Statistical significance was determined using ANOVA and the Fisher's least significance difference test for all K_{sv} values from each acrylamide quenching experiment. K_{sv} values are expressed as mean values at a 95% confidence level.

3. Results

3.1. CD spectroscopy of Dab-2 N-PTB in detergent micelles

Our original Dab2 N-PTB construct (amino acids 1-241) [20] exhibited poor resolution at the NMR scale and behaved poorly in detergent micelles (data not shown). Therefore, we designed a shorter construct of this region, which included a higher degree of amino acid conservation (amino acids 17-185; Fig. 1a and b) that was more suitable for structural studies with micelles. Phylogenetic analyses indicate that the N-PTB region is a highly conserved module in Dab proteins among lineages (Fig. 1b), suggesting that this region has a comparatively recent common ancestor. To determine whether the shorter Dab2 N-PTB construct conserves its sulfatide- and PtdIns(4,5)P_2-binding properties, we used liposomes that closely resembled physiological membranes. The shorter Dab2 N-PTB construct exhibited similar sulfatide- and PtdIns(4,5)P_2-binding characteristics (Fig. 2a) compared with our previously reported data for the Dab2 N-PTB larger construct [20]. Accordingly, mutations in the corresponding sulfatide and PtdIns(4,5)P_2-binding residues abolished lipid binding (Fig. 2a). Thus, the shorter Dab2 N-PTB construct was functional and is named Dab2 N-PTB from here on for simplicity.

Given the role of Dab2 in membrane targeting, we structurally characterized Dab2 N-PTB in the far- and near-UV CD regions in the presence of detergent micelles (DDM, LMPC, and DPC). As shown in the representative spectra, Dab2 N-PTB is an α/β protein, as observed by the presence of bands at 190 and 208 and a slight shoulder at 222 nm (Fig. 2b). Addition of the detergent micelles did not lead to changes in the secondary structure content of the protein when characterized by far-UV (Fig. 2b and Table 1). However, near-UV CD analysis, which measures chirality around aromatic residues providing information about tertiary structure, indicates that the protein had changed its tertiary structure in the presence of either LMPC or DPC micelles (Fig. 2c). Moreover, Dab2 N-PTB exhibited poorly resolved peaks at the NMR scale in the presence of these detergents (data not shown). On the other hand, the tertiary structure of Dab2 N-PTB was conserved in the presence of 0.25 mM DDM (Fig. 2c and Fig. S1) (CMC = 0.18 mM; [35]), a result that supports the use of this micellar system as a membrane mimic for our structural studies.

3.2. Dab2 N-PTB lipid-binding properties

To examine the structural perturbations of the backbone residues that occur upon binding to micelles and lipid ligands, the Dab2 N-PTB region was ^{15}N-labeled and ^{15}N, ^{1}H HSQC spectra were recorded. This NMR experiment was collected in two dimensions, where each amino acid (except proline) results in one signal (chemical shift) that corresponds to the N – H amide group of the backbone residues as well as the N – H side chains of tryptophan, glutamine, and asparagine. These chemical shifts can be tracked by perturbations in their chemical environments to interactions with physiological ligands or even changes in structure or dynamics. The scatter of the NMR backbone resonances of N-PTB is consistent with a structure rich in β-sheets and helices. There are ~158 strong, resolved peaks, representing the majority of the expected 166 backbone ^{15}N– ^{1}H groups in Dab2 N-PTB. Addition of DDM micelles induced line broadening of several resonances (Fig. S1), consistent with the formation of a protein-micelle slower tumbling complex (the molecular mass of DDM micelles ranges between 56 and 72 kDa; [35]). Nonetheless, the overall spectrum of the protein exhibits the same chemical shift dispersion, indicative that the protein retains its overall structure, which is consistent with our CD studies (Fig. 2b and c). The ligand interactions of Dab2 N-PTB were investigated using two-dimensional NMR spectroscopy. Addition of sulfatides embedded in DDM micelles caused a further decrease in resonance intensity, which may indicate that sulfatides increase the affinity of the protein to micelles (Fig. 3a). A soluble form of PtdIns(4,5)P_2 binds to Dab2 N-PTB in a fast exchange regime (Fig. 3b), a result that is consistent with the phosphoinositide-binding properties of the mouse Dab1 PTB domain [17]. Curiously, the addition of c6-PtdIns(4,5)P_2 to Dab2 N-PTB in DDM micelles reversed the line broadening effects induced by micelles and only selective line broadening of resonances was detected (Fig. 3c). Nonetheless, PtdIns(4,5)P_2-enriched DDM micelles induced chemical shift perturbations of the Dab2 N-PTB region that were indistinguishable to those observed with the free phosphoinositide, indicating that the detergent is capable of maintaining the native-like function of the protein.

Our previous studies indicate that Dab2 N-PTB requires Lys53 to bind to both sulfatides and PtdIns(4,5)P_2 [20]. Given the possibility that both lipids could be found simultaneously in the same membrane compartment, we asked whether sulfatides and PtdIns(4,5)P_2 compete with each other for binding to Dab2 N-PTB using a protein–lipid overlay competition assay. Pre-incubation of the Dab2 N-PTB with a 10-molar fold excess of PtdIns(4,5)P_2 reduced sulfatide binding by at least 60% (Fig. 4a). This observation was further confirmed by competing sulfatides and PtdIns(4,5)P_2 for Dab2 N-PTB binding using SPR. Pre-incubation of Dab2 N-PTB with PtdIns(4,5)P_2 reduced protein sulfatide-binding with an IC_{50} of ~10.1 μM (Fig. 4b).

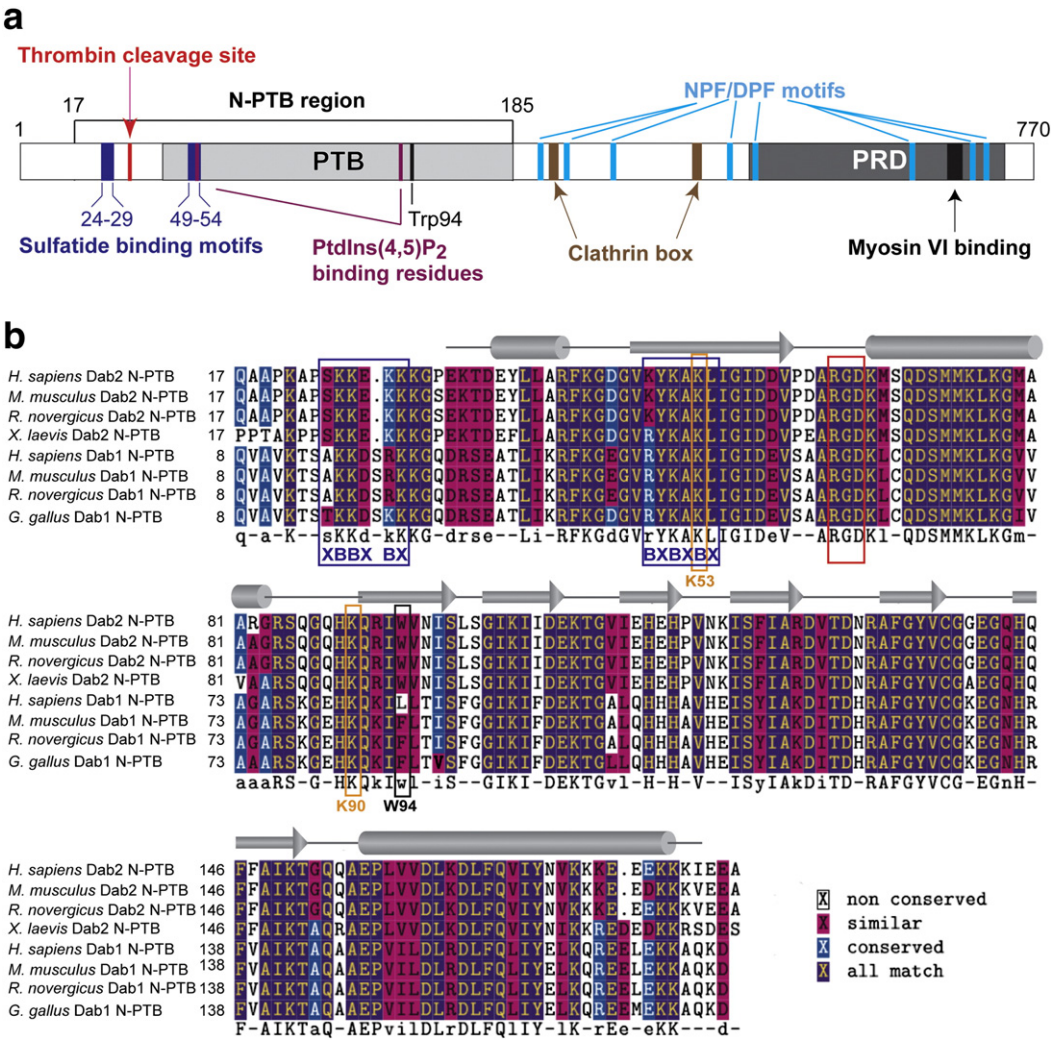

Fig. 1. Modular organization and lipid-binding residues of Dab2. (a) Schematic representation of the Dab2 primary structure with the boundaries of each of the key lipid- and protein-binding regions indicated at the bottom. The NPF and DPF represent the Asn-Pro-Phe and Asp-Pro-Phe motifs, respectively. The red arrow indicates the putative thrombin cleavage site. PRD: proline-rich domain. (b) Sequence alignment of the N-PTB region of the following proteins: *Homo sapiens* Dab2 (Genbank entry AAF23161.1), *Mus musculus* Dab2 (Genbank entry AAG44669.1), *Ratus novergicus* Dab2 (Genbank entry NP_077073), *Xenopus laevis* Dab2 (Genbank entry ABC96762.1), *Homo sapiens* Dab1 (Genbank entry AAH67445.1), *Mus musculus* Dab1 (Genbank entry NP_796233.2), *Ratus novergicus* Dab1 (Genbank entry NP_705885), *Gallus gallus* Dab1 (Genbank entry NP_989569.1). The secondary structural elements determined for the mouse Dab2 PTB domain is shown on top of the sequence alignment. The conserved XBBXBX and BXBXBX sulfatide-binding motifs are boxed. The RGD motif, responsible for integrin binding, is boxed in red. Residues Lys53 and Lys90, engaged in PtdIns(4,5)P_2 recognition, are boxed in orange. The conserved Trp94, a residue used in the fluorescence experiments, is boxed in black.

Taken together, this data suggests that sulfatide- and PtdIns(4,5)P_2-binding sites overlap in Dab2 N-PTB.

3.3. Structural features of Dab2 N-PTB induced by sulfatides

Since Dab2 proteins present a single and conserved Trp residue (Trp94; Fig. 1b and 4c) in their N-PTB region, the fluorescence of its side chain can be used as a chromophore, thus, providing information about changes in its local environment. The fluorescence spectrum of Dab2 N-PTB exhibits a maximum at ~343 nm, indicative that Trp94 resides on the protein surface (Fig. 5a). The protein spectrum remains unchanged after adding DDM micelles, indicating the absence of local conformational changes around Trp94 under these conditions. In the presence of sulfatides, however, the protein fluorescence intensity is increased, indicative that Trp94 becomes less solvent-exposed (Fig. 5a). This change in spectrum is not due to direct contact of Trp94 to sulfatides since mutation of this residue to leucine did not affect sulfatide binding (Fig. 2a). Rather, it may be a consequence of a conformational change of the protein. The conformation of Dab2 N-PTB in the absence and presence of sulfatides was assessed by far- and near-UV CD analyses. Incubation of Dab2 N-PTB with an excess of sulfatide-enriched DDM micelles resulted in minor changes in the far-UV CD spectra (Fig. 5b and Table 1). The near-UV CD spectrum exhibited a more negative signal after the addition of an excess of sulfatide-enriched micelles (Fig. 5c). Signals in the 250–270 nm region are generally associated with Phe, whereas those at 270–290 nm and 280–300 nm are generally attributed to Tyr and Trp, respectively. The Dab2 N-PTB region contains 6 Phe, 4 Tyr, and 1 Trp (Fig. 1b). Thus, the negative signals from 250 to 270 nm are likely due to changes in the environment of the Phe residues, whereas the two negative peaks at ~278 and ~282 nm likely arise from the Tyr side chains of Dab2 N-PTB (Fig. 5c). Alternatively, the new peak at 282 nm could be a consequence of conformational changes around the Trp94 side chain of the protein.

The accessibility and environment of Trp94 were further examined using the neutral water-soluble fluorescent quencher acrylamide [36]. Stern–Volmer plots were linear under all conditions (data not shown), consistent with dynamic quenching. Fig. 5d shows that

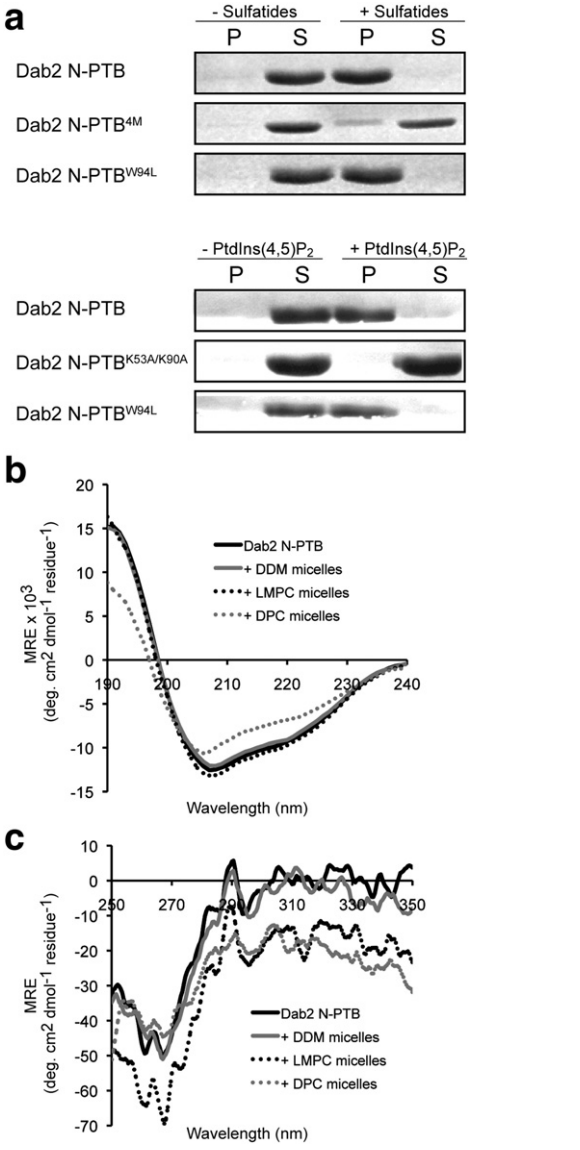

Fig. 2. Function and structure of the Dab2 N-PTB region. (a) The Dab2 N-PTB, N-PTB^{4M}, and N-PTB^{W94L} proteins were incubated with liposomes without and with sulfatides (top panels). The Dab2 N-PTB, N-PTB$^{K53A/K90A}$, and N-PTB^{W94L} proteins were monitored for PtdIns(4,5)P_2-enriched liposome binding (bottom panels). P and S represent pellet and supernatant fractions, respectively, after centrifugation, SDS–PAGE, and coomassie blue staining. (b) Far-UV and (c) Near-UV CD spectra of Dab2 N-PTB in the absence and presence of DDM, DPC, and LMPC micelles. Dab2 N-PTB, N-terminal Dab2 (amino acids 17-185); Dab2 N-PTB^{4M}, Dab2 N-PTB Lys25Ala, Lys49Ala, Lys51Ala, and Lys53Ala; Dab2 N-PTB$^{K53A/K90A}$, Dab2 N-PTB Lys53Ala and Lys90Ala; Dab2 N-PTB^{W94L}, Dab2 N-PTB Trp94Leu.

acrylamide quenched ~90% of the Dab2 N-PTB Trp94 emission signal with an average K_{sv} of 12.9 M^{-1} (Fig. 6), in agreement with the relatively high exposure of this residue to the aqueous environment observed in the mouse Dab2 PTB domain [15]. Addition of DDM micelles significantly reduced acrylamide quenching (Fig. 5e) with an average K_{sv} of 7.9 M^{-1} (Fig. 6). A priori, this result seems to be in contrast to the observed absence of changes in the protein fluorescent spectrum in the presence of micelles (Figs. 5a and 7a). However, an elegant work using Trp octyl ester (TOE) as a Trp-containing protein mimic indicates that the DDM polar headgroup controls the accessibility of TOE to water in detergent micelles [35]. The authors demonstrate that TOE is less accessible to acrylamide quenchers in DDM micelles compared to other micellar systems and that the cohesion of the DDM headgroup plays a role in protecting protein

Table 1
Predicted secondary structure content of Dab2 N-PTB in different detergent micelles and in the absence and presence of sulfatides and PtdIns(4,5)P_2 using the CDSSTR algorithm [31].

Ligand	αR	αD	βR	βD	Turns	Unordered	NRMSD
–	8	10	18	10	23	31	0.012
DDM	8	10	18	11	23	30	0.013
LMPC	8	10	15	10	24	33	0.014
DPC	6	11	17	11	23	32	0.013
DDM/sulfatides	7	7	20	12	23	31	0.033
PtdIns(4,5)P_2	7	9	17	11	24	32	0.021
DDM/PtdIns (4,5)P_2	7	9	16	10	24	34	0.015

function and stability of membrane proteins [35]. We believe that the DDM polar headgroup prevents Dab2 N-PTB Trp94 from being fully in contact with acrylamide, resulting in a reduced K_{sv} value. Remarkably, addition of sulfatides significantly decreased acrylamide quenching (Fig. 5f) as evidenced by a reduced average K_{sv} (4.8 M^{-1}; Fig. 6). Overall, the data suggest that sulfatides contribute to the penetration of Dab2 to membranes by interaction with its N-PTB region.

3.4. Structural features of Dab2 N-PTB induced by PtdIns(4,5)P_2

The structural basis of PtdIns(4,5)P_2-mediated membrane binding of the Dab2 N-PTB region was also investigated. Given the proximity of Trp94 to Lys90 (Fig. 4c), a key PtdIns(4,5)P_2-binding residue [15,20], a lower molar ratio of PtdIns(4,5)P_2 than the sulfatides was needed to track conformational changes in Dab2 N-PTB. Addition of a 4-fold excess of the soluble phosphoinositide quenched the protein fluorescence, suggesting that Trp94 moves to a more hydrophilic environment (Fig. 7a). Addition of PtdIns(4,5)P_2 at a lipid:protein molar ratio higher than 4-fold did not cause further changes in the fluorescent intensity of the protein (data not shown). Far- and near-UV spectra indicate minor structural changes in Dab2 N-PTB upon PtdIns(4,5)P_2 binding (Table 1 and data not shown). This observation indicates that the changes observed in Trp fluorescence are due to local conformational changes of the protein around the aromatic residue upon soluble phosphoinositide binding. The contribution of a membrane mimic in PtdIns(4,5)P_2 recognition was also studied. Addition of the phosphoinositide to the micelle-embedded Dab2 N-PTB did not alter the fluorescent signal of the protein (Fig. 7a). Moreover, no major changes in both secondary and tertiary structures of the protein were observed at the same lipid:protein molar ratio (Fig. 7b and c and Table 1). Acrylamide quenching of the Dab2 N-PTB was slightly reduced by the presence of PtdIns(4,5)P_2 (Fig. 7d), as indicated by a decrease in the average K_{sv} value (10.2 M^{-1}; Fig. 6). The presence of PtdIns(4,5)P_2 in DDM micelles did not contribute to any change in the average K_{sv} value (7.7 M^{-1}) when compared with the protein in DDM micelles (7.9 M^{-1}; Fig. 6). Taken together, these data suggest that PtdIns(4,5)P_2 is not necessary for Dab2 membrane insertion.

3.5. Binding of Dab2 N-PTB to sulfatides and PtdIns(4,5)P_2 increases protein stability

We next tested whether addition of lipid ligands affected the conformational stability of Dab2 N-PTB. CD ellipticity was monitored during thermal unfolding of the protein at 222 nm in the absence and presence of DDM micelles, sulfatides, and PtdIns(4,5)P_2. Thermal denaturation analysis indicated that Dab2 N-PTB exhibits two-state melting transitions, with a highly cooperative unfolding transition between ~35 and 60 °C and an apparent melting temperature (T_m) of 46.6 °C (Fig. 8a and Table S1). The midpoint of the conformational transition was observed to decrease to 40.4 °C in the presence of DDM micelles. Thus, DDM-induced local conformational changes in

Dab2 N-PTB (Figs. 5c and 7c) may lead to a less stable protein. Interestingly, addition of sulfatides into the DDM-embedded Dab2 N-PTB increased the T_m of the protein to 45.2 °C (Fig. 8a). The sulfatide binding deficient Dab2 N-PTB^{4M} exhibits a similar T_m value to that observed for the wild-type protein (46 °C), but becomes remarkably less stable in the presence of DDM micelles (T_m = 36.7 °C; Fig. 8b and Table S1). Importantly, mutations in the sulfatide-binding site did not alter their far-UV circular dichroism spectra compared to wild-type Dab2 N-PTB [20], indicating that the substitutions do not perturb the secondary structure of the protein. Further addition of sulfatides, however, did not contribute to Dab2 N-PTB^{4M} stability as indicated by its T_m value (34.2 °C; Fig. 8b and Table S1). Taken together, these data suggest that sulfatide-binding increases the stability of Dab2 N-PTB. Likewise, PtdIns(4,5)P_2 increased the Dab2 N-PTB's thermal stability with an estimated T_m value of 48.1 °C (Fig. 8c and Table S1). This increase of protein stability was also observed when the phosphoinositide was embedded in DDM micelles, changing the T_m value from 40.4 to 42.2 °C (Fig. 8c and Table S1). Accordingly, mutations in the two critical PtdIns(4,5)P_2-binding residues (Lys53 and Lys90) impaired the protein to increase its tolerance to temperature-induced unfolding in the presence of the phosphoinositide (Fig. 8d and Table S1). This result is not a consequence of a perturbation of the structure of Dab2 N-PTB since alanine substitutions for Lys53 and Lys90 do not disturb its secondary structure [20]. Thus, stabilization of Dab2 N-PTB by PtdIns(4,5)P_2 is a consequence of direct contact of the protein with the phosphoinositide.

4. Discussion

Peripheral proteins, such as Dab2, exhibit weak and reversible membrane binding. To perform this function, Dab2 recognizes sulfatides and phosphoinositides through binding sites located within its N-PTB region [20]. To better understand the mechanism by which Dab2 interacts with membranes, we have screened micelles that are commonly used to study membrane-binding proteins. Here, we show that the structure and function of Dab2 are preserved in DDM micelles (Figs. 2 and 3). DDM micelles have been used to successfully purify membrane proteins for NMR studies [37], to preserve protein activity [38], and to study membrane-binding proteins [39,40].

In hemostasis, it is well established that sulfatides serve as ligands for several proteins such as P-selectin, vWF, and Dab2, to modulate platelet adhesion and aggregation events [20,24]. Upon platelet activation, membrane sulfatides not only sequester Dab2 for integrin binding but also facilitate Dab2 internalization in platelets, thus, protecting it from thrombin cleavage [20]. Furthermore, sulfatide-bound Dab2 not only reduces the number and size of platelet aggregates but also diminishes platelet P-selectin surface levels with a concomitant reduction of P-selectin-mediated cell-cell interactions, which are usually triggered upon platelet activation [27]. Our data indicate that sulfatide binding can be detected by NMR, in which Dab2 N-PTB forms a complex with sulfatide-embedded DDM micelles that resulted in loss of resonance intensity (Fig. 3a). The ability of sulfatides to be recognized by numerous proteins has been associated with the presence of basic amino acid clusters, including the XBBXBX (where B is a basic residue) and BXBXBX motifs [41]. We have identified critical Dab2 N-PTB residues that specifically bind to sulfatides and are located at two conserved sulfatide-consensus motifs (Fig. 2a and [20]), which closely resemble those described in other hemostatic proteins, including laminin-1 [42] and vWF [43].

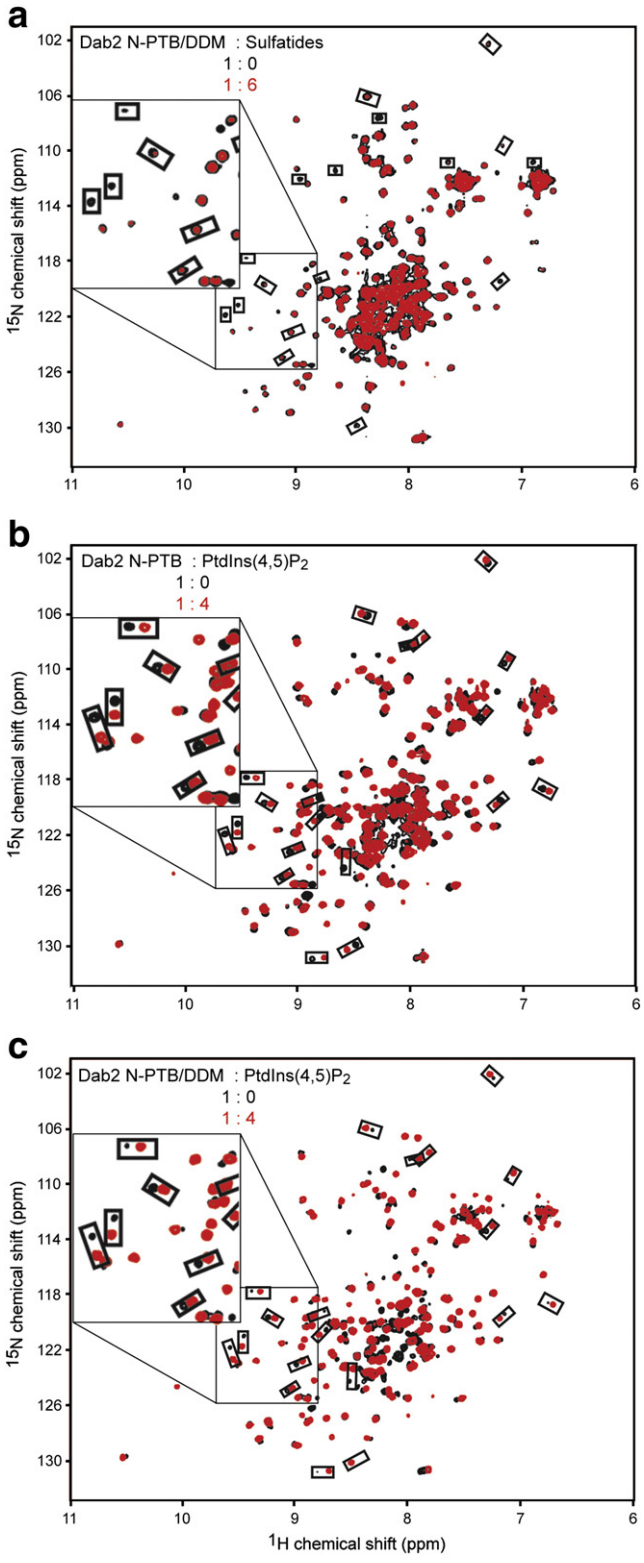

Fig. 3. Dab2 N-PTB is functional in DDM micelles at the NMR scale. (a) DDM-enriched ^{15}N-labeled Dab2 N-PTB (black) was subjected to ^{15}N-HSQC analysis following addition of sulfatide-enriched DDM micelles (1:6 molar ratio; red). Resonances that exhibit reduced intensity are boxed. Several resonances are particularly broadened and perturbed by DDM micelles. Therefore, a lower contour level (4-fold) was used to depict the severely broadened resonances caused by the addition of the detergent. (b) An HSQC spectrum of ^{15}N-labeled Dab2 N-PTB was collected in the absence (black) and presence of c6-PtdIns(4,5)P_2 (1:4 molar ratio; red). Perturbed chemical shifts are boxed. (c) An HSQC spectrum of DDM-enriched ^{15}N-labeled Dab2 N-PTB was collected in the absence (black) and presence of PtdIns(4,5)P_2-enriched DDM micelles (1:4 molar ratio; red). Perturbed chemical shifts are boxed. A lower contour level (4-fold) was used (compared to the NMR spectrum of Dab2 N-PTB shown in panel *a*) to depict the severely broadened resonances caused by the addition of the detergent.

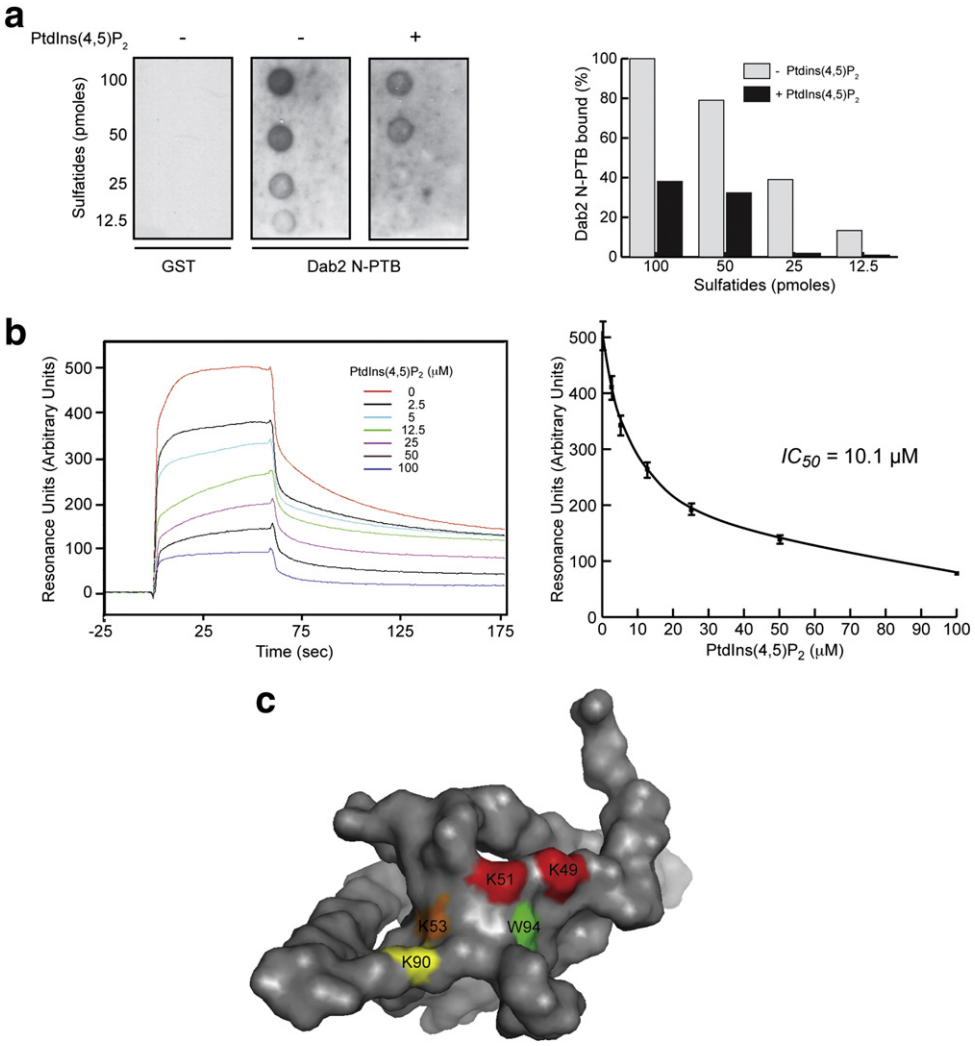

Fig. 4. The sulfatide- and PtdIns(4,5)P_2-binding sites overlap in Dab2 N-PTB. (a) Sulfatide-bound spotted membranes were incubated with either free- or PtdIns(4,5)P_2-bound GST-Dab2 N-PTB. Quantification of the spots (right) was carried out using an AlphaImager. The figure shows data from a single experiment that was repeated three times with similar results. (b) Sulfatide-enriched liposomes were immobilized onto an SPR L1 sensor chip and Dab2 N-PTB (5 μM) was pre-incubated and loaded in the absence and presence of increasing concentrations of PtdIns(4,5)P_2 (left). Data was processed using BioDataFit (right) and they are representative of two independent experiments. (c) A view of the predicted tertiary structure of the human Dab2 PTB domain reproduced from the AL2TS site (http://proteinmodel.org/AS2TS/al2ts.html) using the mouse Dab2 PTB domain (PDB ID: 1M7E) as a template and depicted using Pymol. Experimentally determined sulfatide- (red), PtdIns(4,5)P_2- (yellow) and both lipid- (orange) binding residues are labeled on the protein surface. The location of residue W94 is displayed in green.

A few recent studies have shown structural insights of sulfatide-binding proteins. The antigen-presenting human CD1 is a transmembrane protein known to bind sphingolipids, such as sulfatides, which are presented as antigens for the T-cell receptors during the immune response [44]. The crystal structure of several CD1 proteins indicate that van der Waals contacts, rather than hydrogen bonds, play a major role in the interaction with sphingolipids [23]. Micelles enriched with sulfatides were successfully employed to investigate the membrane-binding mechanism of Cobra Cardiotoxin (CTX) using NMR spectroscopy [45]. Data indicate that the sulfatide head group undergoes conformational changes from a bent shovel to an extended conformation upon CTX binding [45]. Similar to our proposed mechanism of Dab2 recognition to membrane sulfatides, the three-dimensional structure of the CTX-sulfatide complex in $C_{10}E_6$ detergent indicates that CTX penetrates membrane bilayers in a sulfatide-dependent manner by a mechanism that requires both CTX and sulfatide conformational changes to allow the peptide to oligomerize at the membrane bilayer interface [46].

PtdIns(4,5)P_2 is the most abundant phosphoinositide at the plasma membrane (1% of the total lipids; [47]) and plays a key role as a precursor to cellular second messengers and acts as a signaling lipid. While it is well documented that PtdIns(4,5)P_2 is found at the inner leaflet of the plasma membrane [48], recent findings indicate that certain phosphoinositides are also present in the outer leaflet of the plasma membrane of plant and animal cells, which are required for pathogen protein effector entry in a mechanism that depends on the presence of RXLR and dEER conserved lipid-interacting motifs [18]. Therefore, it is possible that sulfatides and phosphoinositides can co-localize at the cell membrane surface. Dab proteins can bind phosphoinositides at the inner leaflet of the plasma membrane through their PTB domain [2,49]. Among phosphoinositides, the Dab PTB domain preferentially binds PtdIns(4,5)P_2, although PtdIns(3,4,5)P_3 has also been suggested to be a physiological ligand [17]. Dab2 is proposed to participate in lipoprotein receptors sorting into clathrin-coated pits that are required for endocytosis [2–4]. PtdIns(4,5)P_2 is also critical for endocytosis since it may be clustered in lipid raft regions of the plasma membrane [15] where Dab2 resides. Notably, Dab2 is abundant in platelets [8] but the role of the protein in recognizing platelet PtdIns(4,5)P_2 still remains elusive. PtdIns(4,5)P_2 contributes to platelet function, including platelet shape [50] and

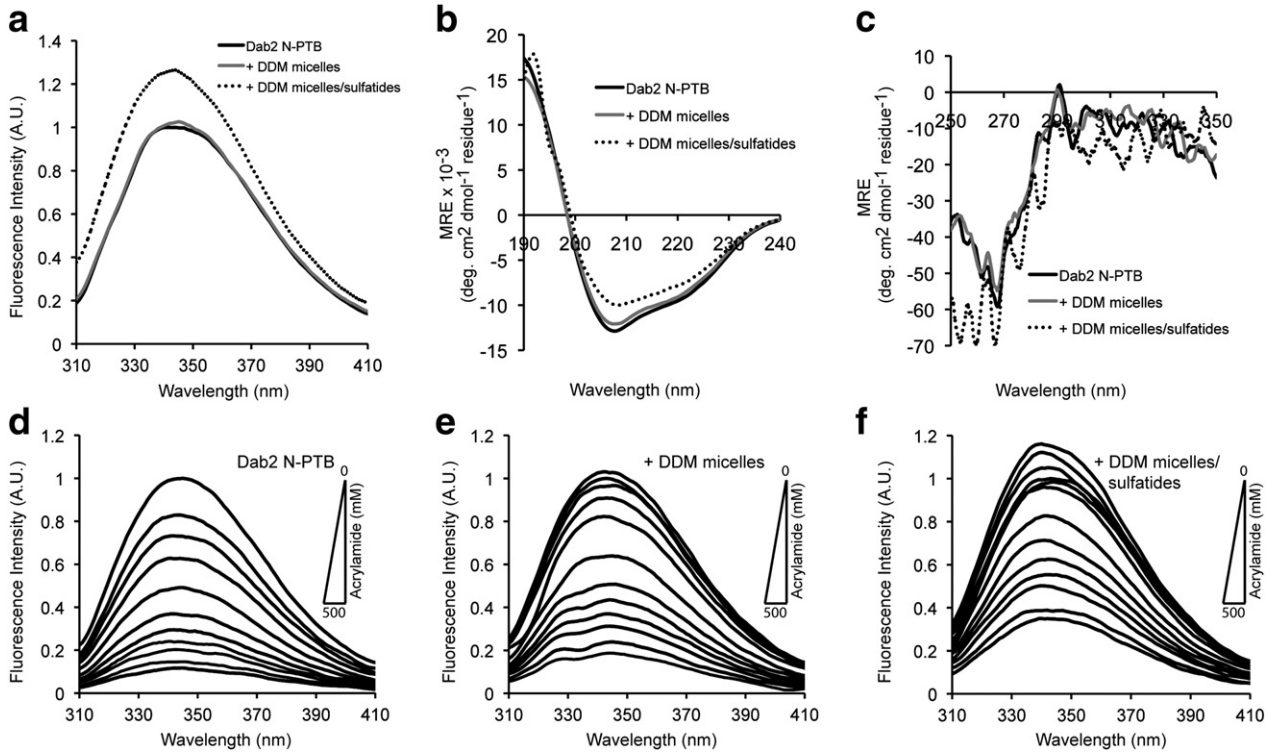

Fig. 5. Biophysical characterization of the association of Dab2 N-PTB to sulfatide-enriched micelles. (a) Tryptophan fluorescence, (b) Far-UV CD, and (c) Near-UV CD spectra of Dab2 N-PTB in the absence (black solid line) and presence of DDM micelles (gray solid line) or sulfatide-enriched DDM micelles (128:1 sulfatide:protein molar ratio; black dotted line). (d–f) Intrinsic Trp quenching of Dab2 N-PTB in the absence (d) and presence of DDM micelles (e) or sulfatide-enriched DDM micelles (f) followed by the addition of increasing concentrations of acrylamide.

spreading [51], and increases its levels by 10–40% at the membrane upon platelet activation [50,52–54]. Notably, PtdIns(4,5)P_2 mediates α-granule secretion [55] and concentrates at the membrane upon integrin receptor activation [54]. Since cytosolic phosphorylated Dab2 has been shown to bind to the β3 subunit of the integrin receptor [19], we speculate that PtdIns(4,5)P_2 docks cytosolic Dab2 at the platelet membrane facilitating its endocytic function. Both Dab2 Lys53 and Lys90 exhibit critical roles for PtdIns(4,5)P_2 recognition (Fig. 2a and [20]). Since phosphoinositide binding is mediated by electrostatic interactions, a small number of Dab1 residues are engaged in lipid recognition [17]. Indeed, we observed a set of chemical shift perturbations in the Dab2 N-PTB NMR spectra after addition of PtdIns(4,5)P_2 (Fig. 3b–c) without a drastic conformational change in the protein (Fig. 7). We also found that sulfatides and PtdIns(4,5)P_2 competed with each other for binding the Dab2 N-PTB region. This finding was expected given the proximity of their binding sites (Fig. 4c) and the fact that Lys53 is shared between these two lipids [20]. On the other hand, the PTB domain of Dab1 and Dab2 is able to simultaneously bind to different ligands, PtdIns(4,5)P_2 and an ApoER2 peptide, through independent sites located in opposite regions in the protein domain [2,16].

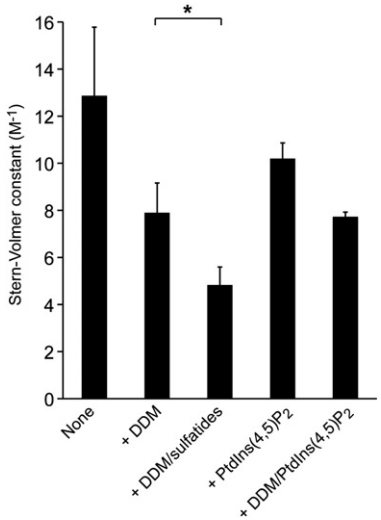

Fig. 6. Stern–Volmer calculations of the acrylamide quenching response of Dab2 N-PTB under the indicated experimental conditions. The correlation coefficients for each calculation ranged from 0.985 to 0.995. *, $P<0.04$.

Tryptophan fluorescence is sensitive to the environment polarity around Trp residues. A reduction in fluorescence emission indicates that the tryptophans come into more contact with the aqueous solution. In all Dab2 proteins, the N-PTB region presents a conserved Trp residue (Trp94; Fig. 1). We found intrinsic protein fluorescence useful in our studies because Trp94 is located near the Dab2 N-PTB sulfatide- and PtdIns(4,5)P_2-binding sites, which makes Trp fluorescence very sensitive to local conformational rearrangements. Fluorescence data show a maximum emission wavelength for Dab2 N-PTB at 343 nm (Figs. 5 and 7). A maximum fluorescent emission of a protein at ~325 nm is usually associated with a Trp residue able to form a hydrogen bond to a water molecule, whereas a maximum at ~347 nm, close to that observed for the Dab2 N-PTB, corresponds to a Trp residue being exposed to a polar solvent [56]. Indeed, the accessibility to the acrylamide quencher is consistent with a relatively polar environment for Trp94 in Dab2 N-PTB. The average K_{sv} value of the free protein was 12.9 M^{-1}, close to the value of the free Trp in solution [57]. Unlike PtdIns(4,5)P_2, sulfatides promoted a conformational change in Dab2 N-PTB that led to an increase in fluorescent

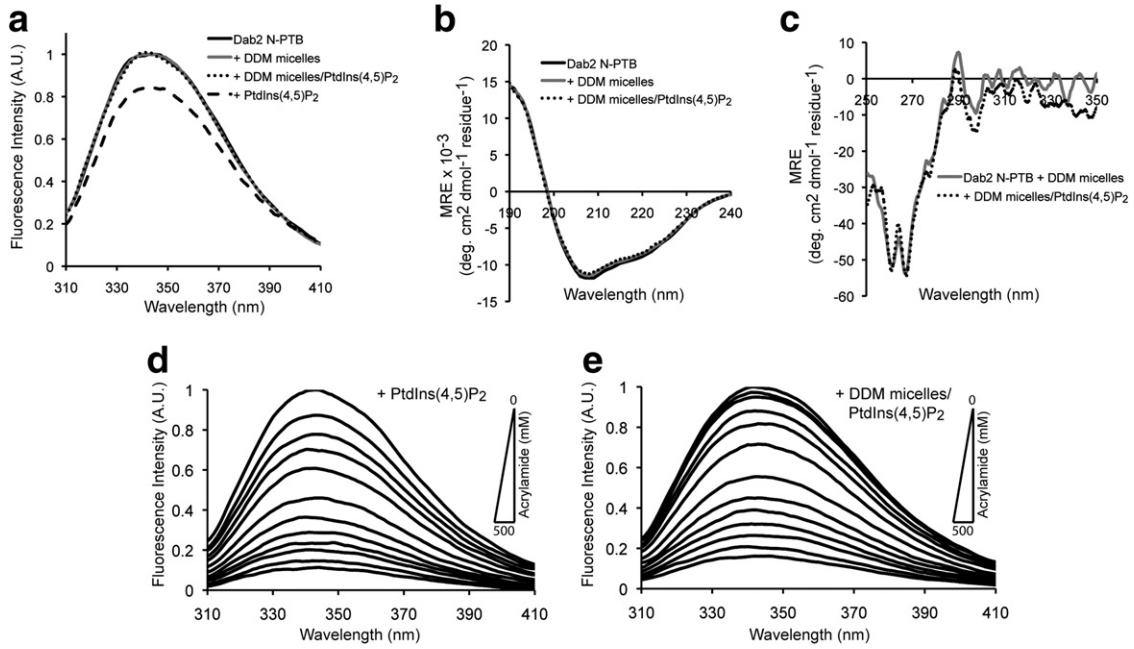

Fig. 7. Biophysical characterization of the association of Dab2 N-PTB to PtdIns(4,5)P_2-enriched micelles. (a) Tryptophan fluorescence, (b) Far-UV CD, and (c) Near-UV CD spectra of Dab2 N-PTB in the absence (black solid line) and presence of soluble PtdIns(4,5)P_2 (black broken line), DDM micelles (gray solid line) or PtdIns(4,5)P_2-enriched DDM micelles (black dotted line). (d–e) Intrinsic Trp quenching of Dab2 N-PTB in complex with soluble PtdIns(4,5)P_2 (d) or PtdIns(4,5)P_2-enriched DDM micelles (e) followed by the addition of increasing concentrations of acrylamide.

intensity, which indicates that the microenvironment surrounding the Dab2 N-PTB Trp94 indole side chain becomes more hydrophobic in sulfatide-embedded micelles. These findings correlate with the observed reduction of the K_{SV} value of the protein in the presence of sulfatides consistent with an altered accessibility of Trp94 to the acrylamide quencher (Figs. 5F and 6). Alteration of quencher

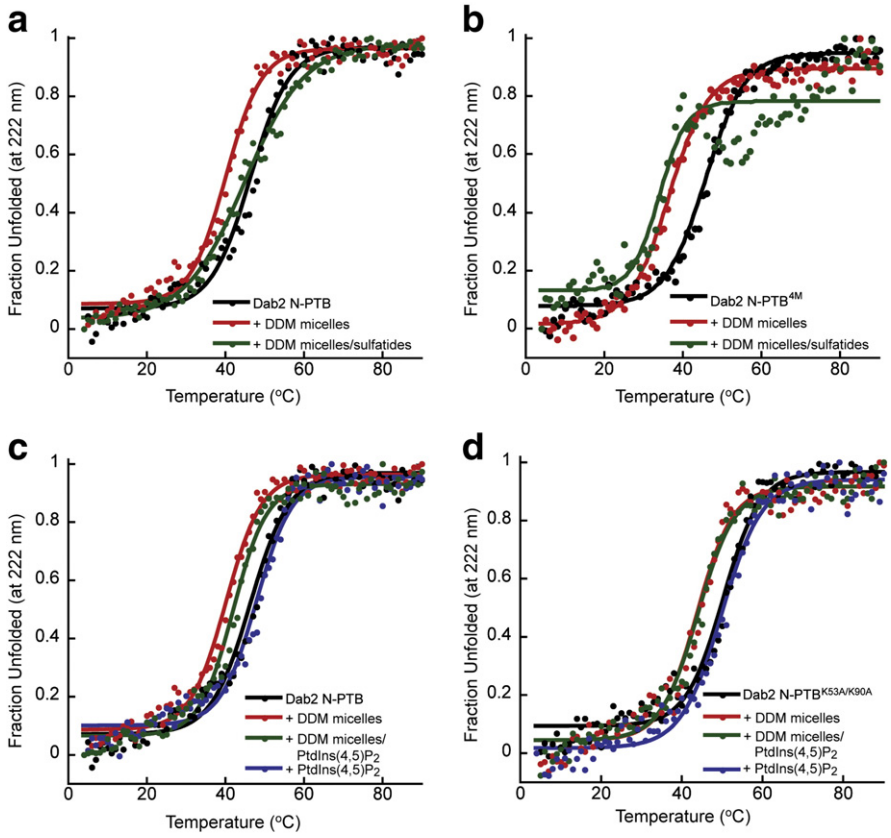

Fig. 8. Lipid-mediated stability of Dab2 N-PTB. (a) CD monitoring of the thermal unfolding of Dab2 N-PTB in the absence (black) and presence of DDM micelles (red), or sulfatide-enriched DDM micelles (green). (b) Same as (a) but using Dab2 N-PTB^{4M}. (c) CD monitoring of the thermal unfolding of Dab2 N-PTB in the absence (black) and presence of soluble PtdIns(4,5)P_2 (blue), DDM micelles (red), or PtdIns(4,5)P_2-enriched DDM micelles (green). (d) Same as (c) but using Dab2 N-PTB$^{K53A/K90A}$.

accessibility is not significant when Dab2 N-PTB is in contact with PtdIns(4,5)P_2-embedded micelles (Fig. 6). However, our thermal denaturation analysis of Dab2 N-PTB suggests that both sulfatides and PtdIns(4,5)P_2 favor stabilization of the protein when embedded in micelles (Fig. 8). This result is similar to that observed for the prokaryotic potassium channel KcsA protein when embedded in DDM micelles, in which the thermal stability is also increased with anionic phospholipids [58]. Thus, it is possible that conformational changes occur in Dab2 N-PTB in the presence of sulfatides, which allows the protein to increase its tolerance to temperature-induced unfolding. Since PtdIns(4,5)P_2 does not induce drastic Dab2 N-PTB conformational rearrangements, these changes must occur locally in regions far from where Trp94 is located, given the absence of changes in fluorescent intensity and in secondary and tertiary structural changes of the protein in the presence of PtdIns(4,5)P_2-enriched micelles (Fig. 7a–c). Taken together, these results suggest that sulfatides, but not PtdIns(4,5)P_2, contribute to Dab2 conformational rearrangement and membrane insertion. Indeed, the proposed sulfatide-mediated insertion of Dab2 in membrane bilayers favors our initial model, in which Dab2 interacts with membrane sulfatides, which unlike PtdIns(4,5)P_2, promotes a protection of Dab2 from thrombin cleavage during platelet activation events [20]. Since Dab PTB domains are able to interact with inositol 1,4,5-triphosphate, the PtdIns(4,5)P_2 head group [15], Dab2 may require contact with the head group of the phosphoinositide to anchor to the plasma membrane, whose association may be critical for Dab2 involvement in clathrin-mediated endocytosis.

5. Conclusions

The significance of this investigation relies on the basis by which Dab2 interacts with membrane bilayers in a lipid-mediated fashion. Despite the overlap of sulfatide- and PtdIns(4,5)P_2-binding sites in Dab2 N-PTB and the fact that both lipids aid in the stabilization of the protein at the membrane, we observed differences in their mechanism of recognition. Whereas sulfatides contributed to Dab2 membrane insertion, which is likely accompanied by a conformational change of the protein, the phosphoinositide contacts a select group of Dab2 residues without additional major changes in the protein structure. Thus, these findings demonstrate the versatility of Dab2 in a wide range of lipid-mediated cellular functions as diverse as platelet aggregation and endocytic events.

Supplementary materials related to this article can be found online at doi:10.1016/j.bbamem.2011.07.029.

Acknowledgements

We are grateful to Dr. Kae-Jung Hwang for her contribution in the initial phase of this work and Dr. Janet Webster for assistance during the preparation of the manuscript. This work was supported by both the Virginia Bioinformatics Institute/Fralin Life Science Institute Core Resources/Equipment Exploratory (to D.G.S.C. and C.V.F.) and the American Heart Association (to D.G.S.C.) grants.

References

[1] F.B. Gertler, R.L. Bennett, M.J. Clark, F.M. Hoffmann, *Drosophila* abl tyrosine kinase in embryonic CNS axons: a role in axonogenesis is revealed through dosage-sensitive interactions with disabled, Cell 58 (1989) 103–113.
[2] S.K. Mishra, P.A. Keyel, M.J. Hawryluk, N.R. Agostinelli, S.C. Watkins, L.M. Traub, Disabled-2 exhibits the properties of a cargo-selective endocytic clathrin adaptor, EMBO J. 21 (2002) 4915–4926.
[3] S.M. Morris, J.A. Cooper, Disabled-2 colocalizes with the LDLR in clathrin-coated pits and interacts with AP-2, Traffic 2 (2001) 111–123.
[4] S.M. Morris, S.D. Arden, R.C. Roberts, J. Kendrick-Jones, J.A. Cooper, J.P. Luzio, F. Buss, Myosin VI binds to and localises with Dab2, potentially linking receptor-mediated endocytosis and the actin cytoskeleton, Traffic 3 (2002) 331–341.
[5] B.A. Hocevar, A. Smine, X.X. Xu, P.H. Howe, The adaptor molecule Disabled-2 links the transforming growth factor beta receptors to the Smad pathway, EMBO J. 20 (2001) 2789–2801.
[6] C. Prunier, P.H. Howe, Disabled-2 (Dab2) is required for transforming growth factor beta-induced epithelial to mesenchymal transition (EMT), J. Biol. Chem. 280 (2005) 17540–17548.
[7] W.T. Chao, J. Kunz, Focal adhesion disassembly requires clathrin-dependent endocytosis of integrins, FEBS Lett. 583 (2009) 1337–1343.
[8] C.L. Huang, J.C. Cheng, A. Stern, J.T. Hsieh, C.H. Liao, C.P. Tseng, Disabled-2 is a novel alphaIIb-integrin-binding protein that negatively regulates platelet-fibrinogen interactions and platelet aggregation, J. Cell Sci. 119 (2006) 4420–4430.
[9] D.A. Calderwood, Y. Fujioka, J.M. de Pereda, B. Garcia-Alvarez, T. Nakamoto, B. Margolis, C.J. McGlade, R.C. Liddington, M.H. Ginsberg, Integrin beta cytoplasmic domain interactions with phosphotyrosine-binding domains: a structural prototype for diversity in integrin signaling, Proc. Natl. Acad. Sci. U. S. A. 100 (2003) 2272–2277.
[10] A. Teckchandani, N. Toida, J. Goodchild, C. Henderson, J. Watts, B. Wollscheid, J.A. Cooper, Quantitative proteomics identifies a Dab2/integrin module regulating cell migration, J. Cell Biol. 186 (2009) 99–111.
[11] J.P. DiNitto, D.G. Lambright, Membrane and juxtamembrane targeting by PH and PTB domains, Biochim. Biophys. Acta 1761 (2006) 850–867.
[12] P. van der Geer, T. Pawson, The PTB domain: a new protein module implicated in signal transduction, Trends Biochem. Sci. 20 (1995) 277–280.
[13] M.T. Uhlik, B. Temple, S. Bencharit, A.J. Kimple, D.P. Siderovski, G.L. Johnson, Structural and evolutionary division of phosphotyrosine binding (PTB) domains, J. Mol. Biol. 345 (2005) 1–20.
[14] B.A. Hocevar, F. Mou, J.L. Rennolds, S.M. Morris, J.A. Cooper, P.H. Howe, Regulation of the Wnt signaling pathway by disabled-2 (Dab2), EMBO J. 22 (2003) 3084–3094.
[15] M. Yun, L. Keshvara, C.G. Park, Y.M. Zhang, J.B. Dickerson, J. Zheng, C.O. Rock, T. Curran, H.W. Park, Crystal structures of the Dab homology domains of mouse disabled 1 and 2, J. Biol. Chem. 278 (2003) 36572–36581.
[16] P.C. Stolt, H. Jeon, H.K. Song, J. Herz, M.J. Eck, S.C. Blacklow, Origins of peptide selectivity and phosphoinositide binding revealed by structures of disabled-1 PTB domain complexes, Structure 11 (2003) 569–579.
[17] P.C. Stolt, D. Vardar, S.C. Blacklow, The dual-function disabled-1 PTB domain exhibits site independence in binding phosphoinositide and peptide ligands, Biochemistry 43 (2004) 10979–10987.
[18] S.D. Kale, B. Gu, D.G. Capelluto, D. Dou, E. Feldman, A. Rumore, F.D. Arredondo, R. Hanlon, I. Fudal, T. Rouxel, C.B. Lawrence, W. Shan, B.M. Tyler, External lipid PI3P mediates entry of eukaryotic pathogen effectors into plant and animal host cells, Cell 142 (2010) 284–295.
[19] C.L. Huang, J.C. Cheng, C.H. Liao, A. Stern, J.T. Hsieh, C.H. Wang, H.L. Hsu, C.P. Tseng, Disabled-2 is a negative regulator of integrin alpha(IIb)beta(3)-mediated fibrinogen adhesion and cell signaling, J. Biol. Chem. 279 (2004) 42279–42289.
[20] K.E. Drahos, J.D. Welsh, C.V. Finkielstein, D.G. Capelluto, Sulfatides partition disabled-2 in response to platelet activation, PLoS One 4 (2009) e8007.
[21] I. Ishizuka, Chemistry and functional distribution of sulfoglycolipids, Prog. Lipid Res. 36 (1997) 245–319.
[22] T. Yamashita, A. Hashiramoto, M. Haluzik, H. Mizukami, S. Beck, A. Norton, M. Kono, S. Tsuji, J.L. Daniotti, N. Werth, R. Sandhoff, K. Sandhoff, R.L. Proia, Enhanced insulin sensitivity in mice lacking ganglioside GM3, Proc. Natl. Acad. Sci. U. S. A. 100 (2003) 3445–3449.
[23] C.F. Snook, J.A. Jones, Y.A. Hannun, Sphingolipid-binding proteins, Biochim. Biophys. Acta 1761 (2006) 927–946.
[24] M. Merten, P. Thiagarajan, Role for sulfatides in platelet aggregation, Circulation 104 (2001) 2955–2960.
[25] D.D. Roberts, V. Ginsburg, Sulfated glycolipids and cell adhesion, Arch. Biochem. Biophys. 267 (1988) 405–415.
[26] A. Aruffo, W. Kolanus, G. Walz, P. Fredman, B. Seed, CD62/P-selectin recognition of myeloid and tumor cell sulfatides, Cell 67 (1991) 35–44.
[27] J.D. Welsh, J.J. Charonko, A. Salmanzadeh, K.E. Drahos, H. Shafiee, M.A. Stremler, R.V. Davalos, D.G. Capelluto, P.P. Vlachos, C.V. Finkielstein, Disabled-2 modulates homotypic and heterotypic platelet interactions by binding to sulfatides, Br. J. Haematol. 154 (2011) 122–133.
[28] D.G. Capelluto, T.G. Kutateladze, R. Habas, C.V. Finkielstein, X. He, M. Overduin, The DIX domain targets dishevelled to actin stress fibres and vesicular membranes, Nature 419 (2002) 726–729.
[29] J.M. Boggs, W. Gao, Y. Hirahara, Signal transduction pathways involved in interaction of galactosylceramide/sulfatide-containing liposomes with cultured oligodendrocytes and requirement for myelin basic protein and glycosphingolipids, J. Neurosci. Res. 86 (2008) 1448–1458.
[30] L. Whitmore, B.A. Wallace, DICHROWEB, an online server for protein secondary structure analyses from circular dichroism spectroscopic data, Nucleic Acids Res. 32 (2004) W668–W673.
[31] N. Sreerama, R.W. Woody, Computation and analysis of protein circular dichroism spectra, Methods Enzymol. 383 (2004) 318–351.
[32] F. Delaglio, S. Grzesiek, G.W. Vuister, G. Zhu, J. Pfeifer, A. Bax, NMRpipe — a multidimensional spectral processing system based on Unix pipes, J. Biomol. NMR 6 (1995) 277–293.
[33] D.S. Garrett, R. Powers, A.M. Gronenborn, G.M. Clore, A common-sense approach to peak picking in 2-dimensional, 3-dimensional, and 4-dimensional spectra using automatic computer-analysis of contour diagrams, J. Magn. Reson. B 95 (1991) 214–220.

[34] M. Sweede, G. Ankem, B. Chutvirasakul, H.F. Azurmendi, S. Chbeir, J. Watkins, R.F. Helm, C.V. Finkielstein, D.G. Capelluto, Structural and membrane binding properties of the Prickle PET domain, Biochemistry 47 (2008) 13524–13536.
[35] L. Tortech, C. Jaxel, M. Vincent, J. Gallay, B. de Foresta, The polar headgroup of the detergent governs the accessibility to water of tryptophan octyl ester in host micelles, Biochim. Biophys. Acta 1514 (2001) 76–86.
[36] M.R. Eftink, Fluorescence techniques for studying protein structure, Methods Biochem. Anal. 35 (1991) 127–205.
[37] A. Koglin, C. Klammt, N. Trbovic, D. Schwarz, B. Schneider, B. Schafer, F. Lohr, F. Bernhard, V. Dotsch, Combination of cell-free expression and NMR spectroscopy as a new approach for structural investigation of membrane proteins, Magn. Reson. Chem. 44 (2006) S17–S23 Spec No.
[38] L.Z. Mi, M.J. Grey, N. Nishida, T. Walz, C. Lu, T.A. Springer, Functional and structural stability of the epidermal growth factor receptor in detergent micelles and phospholipid nanodiscs, Biochemistry 47 (2008) 10314–10323.
[39] L. Columbus, J. Lipfert, K. Jambunathan, D.A. Fox, A.Y. Sim, S. Doniach, S.A. Lesley, Mixing and matching detergents for membrane protein NMR structure determination, J. Am. Chem. Soc. 131 (2009) 7320–7326.
[40] H.J. Kim, S.C. Howell, W. Van Horn, Y.H. Jeon, C.R. Sanders, Recent advances in the application of solution NMR spectroscopy to multi-span integral membrane proteins, Prog. Nucl. Magn. Reson. Spectrosc. 55 (2009) 335–360.
[41] R. Sandhoff, H. Grieshaber, R. Djafarzadeh, T.P. Sijmonsma, A.E. Proudfoot, T.M. Handel, H. Wiegandt, P.J. Nelson, H.J. Grone, Chemokines bind to sulfatides as revealed by surface plasmon resonance, Biochim. Biophys. Acta 1687 (2005) 52–63.
[42] S. Li, P. Liquari, K.K. McKee, D. Harrison, R. Patel, S. Lee, P.D. Yurchenco, Laminin-sulfatide binding initiates basement membrane assembly and enables receptor signaling in Schwann cells and fibroblasts, J. Cell Biol. 169 (2005) 179–189.
[43] T. Nakayama, T. Matsushita, K. Yamamoto, N. Mutsuga, T. Kojima, A. Katsumi, N. Nakao, J.E. Sadler, T. Naoe, H. Saito, Identification of amino acid residues responsible for von Willebrand factor binding to sulfatide by charged-to-alanine-scanning mutagenesis, Int. J. Hematol. 87 (2008) 363–370.
[44] E.M. Beckman, S.A. Porcelli, C.T. Morita, S.M. Behar, S.T. Furlong, M.B. Brenner, Recognition of a lipid antigen by CD1-restricted alpha beta+ T cells, Nature 372 (1994) 691–694.
[45] S.C. Tjong, P.L. Wu, C.M. Wang, W.N. Huang, N.L. Ho, W.G. Wu, Role of glycosphingolipid conformational change in membrane pore forming activity of cobra cardiotoxin, Biochemistry 46 (2007) 12111–12123.
[46] C.H. Wang, J.H. Liu, S.C. Lee, C.D. Hsiao, W.G. Wu, Glycosphingolipid-facilitated membrane insertion and internalization of cobra cardiotoxin. The sulfatide. cardiotoxin complex structure in a membrane-like environment suggests a lipid-dependent cell-penetrating mechanism for membrane binding polypeptides, J. Biol. Chem. 281 (2006) 656–667.
[47] S. McLaughlin, D. Murray, Plasma membrane phosphoinositide organization by protein electrostatics, Nature 438 (2005) 605–611.
[48] M.A. Lemmon, Membrane recognition by phospholipid-binding domains, Nat. Rev. Mol. Cell Biol. 9 (2008) 99–111.
[49] B.W. Howell, L.M. Lanier, R. Frank, F.B. Gertler, J.A. Cooper, The disabled 1 phosphotyrosine-binding domain binds to the internalization signals of transmembrane glycoproteins and to phospholipids, Mol. Cell. Biol. 19 (1999) 5179–5188.
[50] J.H. Hartwig, G.M. Bokoch, C.L. Carpenter, P.A. Janmey, L.A. Taylor, A. Toker, T.P. Stossel, Thrombin receptor ligation and activated Rac uncap actin filament barbed ends through phosphoinositide synthesis in permeabilized human platelets, Cell 82 (1995) 643–653.
[51] J.M. Heraud, C. Racaud-Sultan, D. Gironcel, C. Albiges-Rizo, T. Giacomini, S. Roques, V. Martel, M. Breton-Douillon, B. Perret, H. Chap, Lipid products of phosphoinositide 3-kinase and phosphatidylinositol 4,5-bisphosphate are both required for ADP-dependent platelet spreading, J. Biol. Chem. 273 (1998) 17817–17823.
[52] I. Lassing, U. Lindberg, Polyphosphoinositide synthesis in platelets stimulated with low concentrations of thrombin is enhanced before the activation of phospholipase C, FEBS Lett. 262 (1990) 231–233.
[53] C. Racaud-Sultan, G. Mauco, C. Guinebault, M. Plantavid, B. Payrastre, M. Breton, H. Chap, Rapid and transient thrombin stimulation of phosphatidylinositol 4,5-bisphosphate synthesis but not of phosphatidylinositol 3,4-bisphosphate independent of phospholipase C activation in platelets, FEBS Lett. 330 (1993) 347–351.
[54] S. Bodin, C. Soulet, H. Tronchere, P. Sie, C. Gachet, M. Plantavid, B. Payrastre, Integrin-dependent interaction of lipid rafts with the actin cytoskeleton in activated human platelets, J. Cell Sci. 118 (2005) 759–769.
[55] N. Rozenvayn, R. Flaumenhaft, Phosphatidylinositol 4,5-bisphosphate mediates Ca2 + − induced platelet alpha-granule secretion: evidence for type II phosphatidylinositol 5-phosphate 4-kinase function, J. Biol. Chem. 276 (2001) 22410–22419.
[56] Y.K. Reshetnyak, Y. Koshevnik, E.A. Burstein, Decomposition of protein tryptophan fluorescence spectra into log-normal components. III. Correlation between fluorescence and microenvironment parameters of individual tryptophan residues, Biophys. J. 81 (2001) 1735–1758.
[57] M.R. Eftink, C.A. Ghiron, Fluorescence quenching of indole and model micelle systems, J. Phys. Chem. 80 (1976) 486–493.
[58] I. Triano, F.N. Barrera, M.L. Renart, M.L. Molina, G. Fernandez-Ballester, J.A. Poveda, A.M. Fernandez, J.A. Encinar, A.V. Ferrer-Montiel, D. Otzen, J.M. Gonzalez-Ros, Occupancy of nonannular lipid binding sites on KcsA greatly increases the stability of the tetrameric protein, Biochemistry 49 (2010) 5397–5404.